Nuclear Physics B129 (1977) 1–18

NEW INFORMATION ABOUT THE KAON-NUCLEON-HYPERON COUPLING CONSTANTS $g(\bar{K}N\Sigma(1197))$, $g(\bar{K}N\Sigma(1385))$ and $g(\bar{K}N\Lambda(1405))$

O. BRAUN, H.J. GRIMM [1], V. HEPP, H. STRÖBELE, C. THÖL [2] and T.J. THOUW [3]
Institut für Hochenergiephysik der Universität Heidelberg

D. CAPPS, F. GANDINI [4], C. KIESLING [5], D.E. PLANE [6] and W. WITTEK
Max-Planck-Institut für Physik und Astrophysik, München

G. DOSCH and H. ODOJ
Institut für Theoretische Physik der Universität Heidelberg

Received 10 June 1977
(Revised 5 August 1977)

The reactions $K^-d \to \Sigma^-p$, $K^-d \to \Sigma^-(1385)p$, $K^-d \to \Lambda(1405)n$ and $K^-d \to \Lambda(1520)n$ have been studied at K^- momenta between 686 and 844 MeV/c in an experiment with the 81 cm Saclay bubble chamber at CERN. About 630 000 pictures have been analyzed. Partial and differential cross sections are presented. A one-nucleon-exchange model is used to extract the kaon-nucleon-hyperon coupling constants from these results. For $g(\bar{K}N\Sigma(1197))$, $g(\bar{K}N\Sigma(1385))$ and $g(\bar{K}N\Lambda(1405))$ we find values which are compatible with the SU(3) predictions. The coupling constant $g(\bar{K}N\Lambda(1520))$ obtained by our method agrees with that determined from the partial decay width for $\Lambda(1520) \to \bar{K}N$.

1. Introduction

This paper reports on the reactions

$$K^-d \to \Sigma^-p\,, \tag{1}$$

[1] Now at GMD, Bonn.
[2] Now at Saclay, Paris.
[3] Now at Univ. Dortmund.
[4] Now at IBM, Böblingen.
[5] Now at SLAC, Stanford.
[6] Now at CERN, Genève.

$$K^-d \to \Sigma^-(1385)p\,, \qquad \Sigma^-(1385) \to \Lambda\pi^-\,, \tag{2}$$

$$K^-d \to \Lambda(1405)n\,, \qquad \Lambda(1405) \to \Sigma^-\pi^+\,, \tag{3}$$

$$K^-d \to \Lambda(1520)n\,, \qquad \Lambda(1520) \to K^-p\,, \tag{4a}$$

$$K^-d \to \Lambda(1520)n\,, \qquad \Lambda(1520) \to \Sigma^-\pi^+\,, \tag{4b}$$

at K^- momenta between 686 and 844 MeV/c. Partial and differential cross sections are presented. In the framework of the one-nucleon-exchange (ONE) model reactions (1), (2), (3) and (4) are described as the formation of a hyperon: the kaon interacts with only one nucleon which is off mass shell while the other nucleon acts as a spectator. On the basis of this model cross-section measurements for these reactions determine directly the coupling constants for the kaon-nucleon-hyperon vertex. For all hyperons with masses below the $\bar{K}N$ threshold this approach is the only way to get direct experimental information about their coupling to the $\bar{K}N$ system. We have deduced from our differential cross-section measurements new information about the $\bar{K}N\Sigma$, $\bar{K}N\Sigma(1385)$ and $\bar{K}N\Lambda(1405)$ coupling constants. The known $\bar{K}N\Lambda(1520)$ coupling constant was compared to the value obtained by an analysis of reaction (4) to get a quantitative measure of the limitations of our approach.

Details of the experimental procedure can be found in ref. [1]. The data processing of the candidates for reactions (1), (2), (3) and (4) is described in sect. 2 of this paper. Experimental results are presented and discussed in sect. 3. The ONE model used in the analysis is described in sect. 4. The coupling constants derived from the measured differential cross sections and a comparison with SU(3) predictions and other determinations are presented in sects. 5 and 6.

2. Experimental procedure

The K^- beam was tuned to four momenta (686, 738, 788, 844 MeV/c at the entrance window of the bubble chamber) and had less than 2% background from π^- mesons. Approximately 630 000 pictures were analyzed corresponding to a sensitivity of 7 100 events/mb. The film was double scanned and the overall detection efficiency was found to be 99%. All events were predigitized and subsequently measured automatically by an HPD and a PEPR device. Up to two remeasurements were made. For data processing the modified CERN programs THRESH, GRIND and SLICE were used. Geometrical cuts (e.g. for small projected decay angles and short projected lengths of hyperon tracks) were introduced to allow a proper correction for geometrical losses. These losses as well as those due to hyperons decaying outside of the chamber were compensated for by individual weights. An additional global factor corrects for inefficiencies in the scanning, measuring and

Table 1
Numbers of events and correction factors

Reaction	No. of events	Average individual weight	Global correction factor	Average total weight
$K^-d \to \Sigma^-p$	450	1.17	1.04	1.22
$K^-d \to \Lambda\pi^-p$ ($M(\Lambda\pi^-) < 1.5$ GeV)	1712	1.27	1.67	2.12
$K^-d \to \Sigma^-\pi^+n$ ($M(\Sigma^-\pi^+) < 1.58$ GeV)	1824	1.22	1.21	1.48
$K^-d \to K^-pn$ ($M(K^-p) < 1.58$ GeV)	11980	1.055	1.07	1.13

kinematic fitting as well as for neutral decays of hyperons. The weights and correction factors are listed in table 1.

2.1. Selection of events for the reaction $K^-d \to \Sigma^-p$

Candidates for reaction (1) are obtained from the sample of two-prong events with an associated decay of the negative particle. The kinematic fits are in general fourfold constrained. Competing processes like

$$K^-d \to \Sigma^-p\pi^0 ,$$

$$K^-d \to K^-pn ,$$

$$K^-d \to p\pi^-X ,$$

with the negative particle decaying or interacting (all one constrained fits) can normally be separated kinematically. An upper limit in the hyperon lifetime at 4.5 τ and a lower limit in the kaon lifetime removed the remaining ambiguities. Reactions with a π^+ in the final state could be separated by an ionisation decision.

2.2. Selection of events for the reaction $K^-d \to \Lambda\pi^-p$

Candidates for reaction (2) are obtained from the sample of two-prong events with an associated Λ-decay. Ambiguities between $K^-d \to \Lambda\pi^-p$ and $K^-d \to \Sigma^0\pi^-p$ were resolved by studying the correlation between the missing mass MM^2 ($K^-d \to p\pi^-MM$) and the missing energy ME ($K^-d \to p\pi^-\Lambda ME$). Fig. 1 shows the distributions of MM^2 ($K^-d \to p\pi^-MM$) for the separated final $\Lambda\pi^-p$ and $\Sigma^0\pi^-p$ samples, which are well centered and symmetric around the Λ and Σ^0 masses. The contami-

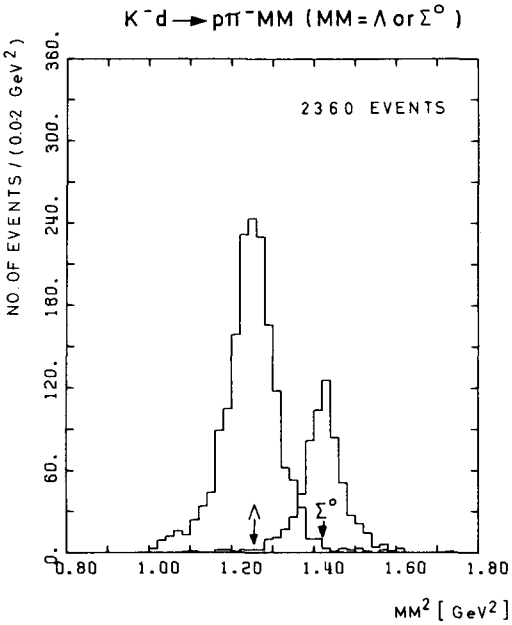

Fig. 1. Distributions of the missing mass squared MM^2 ($K^-d \to p\pi^-MM$) for the final samples of the reactions $K^-d \to \Lambda\pi^-p$ and $K^-d \to \Sigma^0\pi^-p$. The ($\Lambda\pi^-$) mass was restricted to values below 1.5 GeV.

nation of the $K^-d \to \Lambda\pi^-p$ sample by the $\Lambda\pi^+\pi^-n$ final state was found to be negligible.

2.3. Selection of events for the reaction $K^-d \to \Sigma^-\pi^+n$

Candidates for reactions (3) and (4b) are obtained from the sample of two-prong events with an associated decay of the Σ^-. The $\Sigma^-\pi^+n$ final state is easily separated from hypotheses with a proton in the final state. The reaction $K^-d \to \Sigma^-\pi^+n$ was saerched for in only $\frac{2}{3}$ of the film. The reaction $K^-d \to \Sigma^+\pi^-n$ was not used for this analysis as poor resolution in this channel made if difficult to distinguish resonance signal from background.

2.4. Selection of events for the reaction $K^-d \to K^-pn$

Candidates for reaction (4a) are obtained from the sample of those two-prong events where the positive track had been associated with a proton. Any contamination in the K^-pn final state will not contribute to the $\Lambda(1520)$ signal in the invariant mass $M(K^-p)$ except for $K^-pn\pi^0$, which was found to be well separated from the K^-pn final state (see fig. 2).

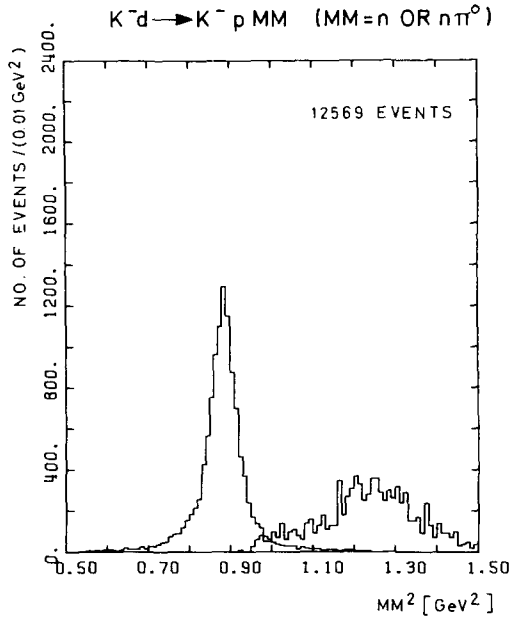

Fig. 2. Distributions of the missing mass squared MM^2 ($K^-d \to K^-pMM$) for the final samples of the reactions $K^-d \to K^-pn$ and $K^-d \to K^-pMM$. The (K^-p) mass was restricted to values below 1.58 GeV. The distribution of the events belonging to the missing mass sample has been scaled by a factor of ten.

2.5. Determination of resonance contributions

The fraction of events of the 3-body final states resulting from the reactions $K^-d \to YN$ at each beam momentum and in each t-interval ($t = (K - Y)^2 = (d - N_{spectator})^2$) was determined by fitting the incoherent sum of relativistic Breit-Wigner distributions and a smooth background to the distribution of the invariant mass

Table 2
Resonance mass, resonance width and order of background polynomial used for the determination of resonance contributions (see subsect. 2.5)

Final state	Resonance	Mass (MeV)	Width (MeV)	Order of background
$\Lambda\pi^-p$	$\Sigma(1385)$	1387	40	1
$\Sigma^-\pi^+n$	$\Lambda(1405)$	1420	40	2
	$\Lambda(1520)$	1515	18	2
K^-pn	$\Lambda(1520)$	1517	18	5 [a]

[a] For $d\sigma/dt$ from this reaction a background of order 2 was found to be sufficient.

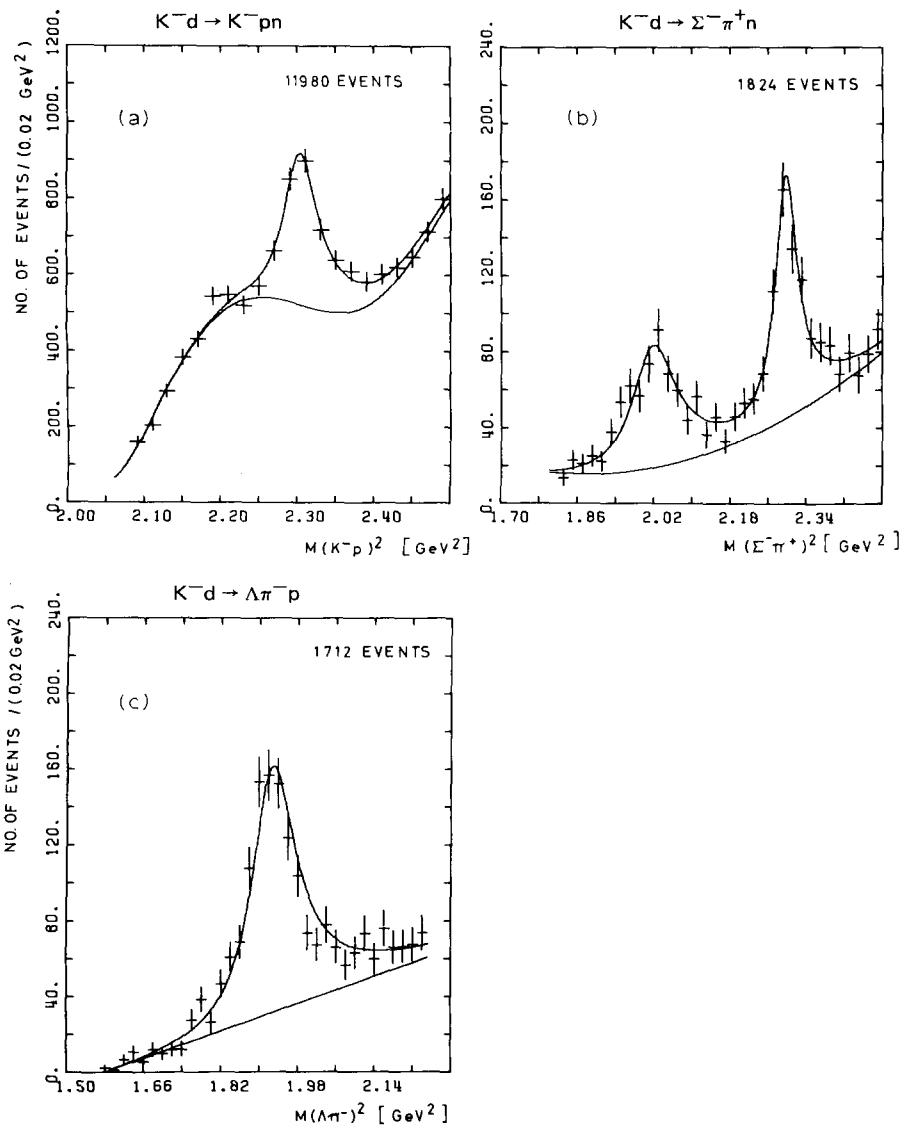

Fig. 3. Distributions of the effective (a) (K^-p) mass in the reaction $K^-d \to K^-pn$; (b) ($\Sigma^-\pi^+$) mass in the reaction $K^-d \to \Sigma^-\pi^+n$; (c) ($\Lambda\pi^-$) mass in the reaction $K^-d \to \Lambda\pi^-p$. The curves represent the results of the fits described in subsect. 2.5.

of the meson-hyperon system (K^-p system for the K^-pn final state). (An energy dependent width for the Breit-Wigner function [2] was used.) The background was parametrized as a sum of Legendre polynomials. The order of the background, as well as the position of the resonances, was found by fitting the total sample of

events from each reaction, the order being the lowest necessary to give an acceptable fit. Thereafter, all fits at different beam momenta and in different t-intervals were made with this mass and the same order in the background parametrization. Only the amount of resonance and the coefficients of the Legendre polynomials was allowed to vary. The relevant parameters are given in table 2 and the corresponding fits to the total sample of events from each reaction are shown in fig. 3.

3. Partial and differential cross sections

The cross sections of reactions (1), (2), (3), (4a) and (4b) have been determined using the number of τ decays and the respective number of events for the various reactions:

$$\sigma = \frac{\text{no. of weighted events}}{\text{no. of } \tau\text{'s}} \times \text{overall correction factor} \times \frac{1}{P_k}\left(\frac{Bm_K}{nc\tau_0}\right) .$$

The constant in brackets (= 1.76 GeV/c · mb) was calculated using a K^- lifetime $\tau_0 = (1.237 \pm 0.0036) \cdot 10^{-8}$ sec, a branching ratio $B = (K^- \to \pi^+\pi^-\pi^-/K^- \to \text{all}) = 0.0559 \pm 0.0003$, a K^- mass $m_K = 0.493707$ GeV and a deuterium density $n = 0.42 \cdot 10^{23}$ deuterons/cm^3. P_k is the average beam momentum in the laboratory system. Each event was weighted as described in sect. 2. A total of 17118 τ-decays was found.

Table 3 gives for the four beam momenta the channel cross sections and the respective numbers of events with and without a t-cut. In table 4 the differential cross sections averaged over the four beam momenta are tabulated.

For reaction (1) the quoted errors include only statistical uncertainties and we estimate the systematic error due to incorrectly identified events to be smaller than 6%. For reaction (2), (3) and (4) the errors given are determined by the fit described in sect. 2.5. In the cross-section calculations the following branching fractions have been used [3]:

$$(\Lambda(1405) \to \Sigma^-\pi^+)/(\Lambda \to \text{all}) = 0.33 ,$$

$$(\Sigma^-(1385) \to \Lambda\pi^-)/(\Sigma^- \to \text{all}) = 0.88 \pm 0.02 ,$$

$$(\Lambda(1520) \to K^-p)/(\Lambda \to \text{all}) = 0.23 \pm 0.005 ,$$

$$(\Lambda(1520) \to \Sigma^-\pi^+)/(\Lambda \to \text{all}) = 0.14 \pm 0.003 .$$

In figs. 4a, b, c, d the differential cross sections for reactions (1), (2), (3) and (4) are shown, along with predictions of the model discussed in the following section.

Table 3
Partial cross sections as a function of the laboratory momentum with and without a t-cut

Lab. momentum (MeV/c)	No. of τ-decays [a]	$K^-d \to \Sigma^-p$		$K^-d \to \Sigma^-(1385)p$ (from $\Lambda\pi^-p$)		$K^-d \to \Lambda(1405)n$ (from $\Sigma^-\pi^+n$)		$K^-d \to \Lambda(1520)n$ (from $\Sigma^-\pi^+n$)		$K^-d \to \Lambda(1520)n$ (from K^-pn)	
		no. of events	$\sigma(\mu b)$	no. of events	$\sigma(\mu b)$	no. of events	$\sigma(\mu b)$	no. of events	$\sigma(\mu b)$	no. of events	$\sigma(\mu b)$
673	4295 (2861)	101	81.2 ± 8.0	235	273 ± 39	165	550 ± 139	166	1349 ± 239	457	1328 ± 271
727	4779 (3113)	142	95.0 ± 8.0	326	315 ± 32	145	411 ± 112	154	1065 ± 215	439	1062 ± 305
778	5110 (3097)	124	70.8 ± 6.4	298	252 ± 30	154	410 ± 100	157	1020 ± 183	421	891 ± 233
834	2934 (1621)	83	79.0 ± 8.7	201	276 ± 38	92	437 ± 91	76	880 ± 213	268	921 ± 116
673–834	17118 (10692)	450	81.5 ± 3.8	1000 [b]	261 ± 18	512 [b]	410 ± 62	492 [b]	960 ± 111	1603 [b]	1048 ± 78
		$0.2 < t < 0.4$ GeV^2		$-0.09 < t < 0.54$ GeV^2						$0.52 < t < 0.71$ GeV^2	
673		24	17.0 ± 3.5	158	183 ± 25					113	328 ± 72
727		35	21.3 ± 3.6	170	164 ± 24					145	351 ± 85
778		24	12.7 ± 2.6	166	140 ± 20					212	449 ± 73
834		14	11.7 ± 3.1	108	148 ± 25					122	419 ± 97

[a] The numbers in brackets refer to that part of the film in which the reaction $K^-d \to \Sigma^-\pi^+n$ has been measured.
[b] Result of the fit to the total sample of events.

Table 4
Differential cross sections as a function of the four-momentum transfer squared $t = (K - Y)^2$

$K^-d \to \Sigma^-p$			$K^-d \to \Sigma^-(1385)p$			$K^-d \to \Lambda(1405)n$		
no. of events	t-range (GeV^2)	$d\sigma/dt$ ($\mu b/GeV^2$)	no. of events	t-range (GeV^2)	$d\sigma/dt$ ($\mu b/GeV^2$)	no. of events	t-range (GeV^2)	$d\sigma/dt$ ($\mu b/GeV^2$)
59	0.35–0.45	118 ± 15	247	0.51–0.61	658 ± 84	90	0.52–0.65	383 ± 95
37	0.25–0.35	66 ± 11	196	0.41–0.51	507 ± 43	43	0.30–0.52	157 ± 80
39	0.15–0.25	69 ± 11	137	0.29–0.41	285 ± 47	36	0.0 –0.30	99 ± 42
29	0.05–0.15	52 ± 9	153	0.14–0.29	266 ± 34			
35	−0.05–0.05	60 ± 10	62	−0.09–0.14	72 ± 24			
22	−0.15–(−0.05)	39 ± 8						
32	−0.25–(−0.15)	58 ± 10						
22	−0.35–(−0.25)	39 ± 8						
20	−0.45–(−0.35)	35 ± 8						
23	−0.55–(−0.45)	41 ± 9						

$K^-d \to \Lambda(1520)n$ (from K^-pn)			$K^-d \to \Lambda(1520)n$ (from $\Sigma^-\pi^+n$)		
no. of events	t-range (GeV^2)	$d\sigma/dt$ ($\mu b/GeV^2$)	no. of events	t-range (GeV^2)	$d\sigma/dt$ ($\mu b/GeV^2$)
145	0.75–0.77	6174 ± 869	148	0.71–0.77	3171 ± 1218
238	0.71–0.75	3983 ± 729	102	0.65–0.71	2987 ± 776
239	0.65–0.71	2677 ± 473	68	0.52–0.65	903 ± 339
179	0.60–0.65	2336 ± 464	53	0.30–0.52	468 ± 163
183	0.52–0.60	1496 ± 322			
94	0.41–0.52	561 ± 228			
68	0.30–0.41	405 ± 175			

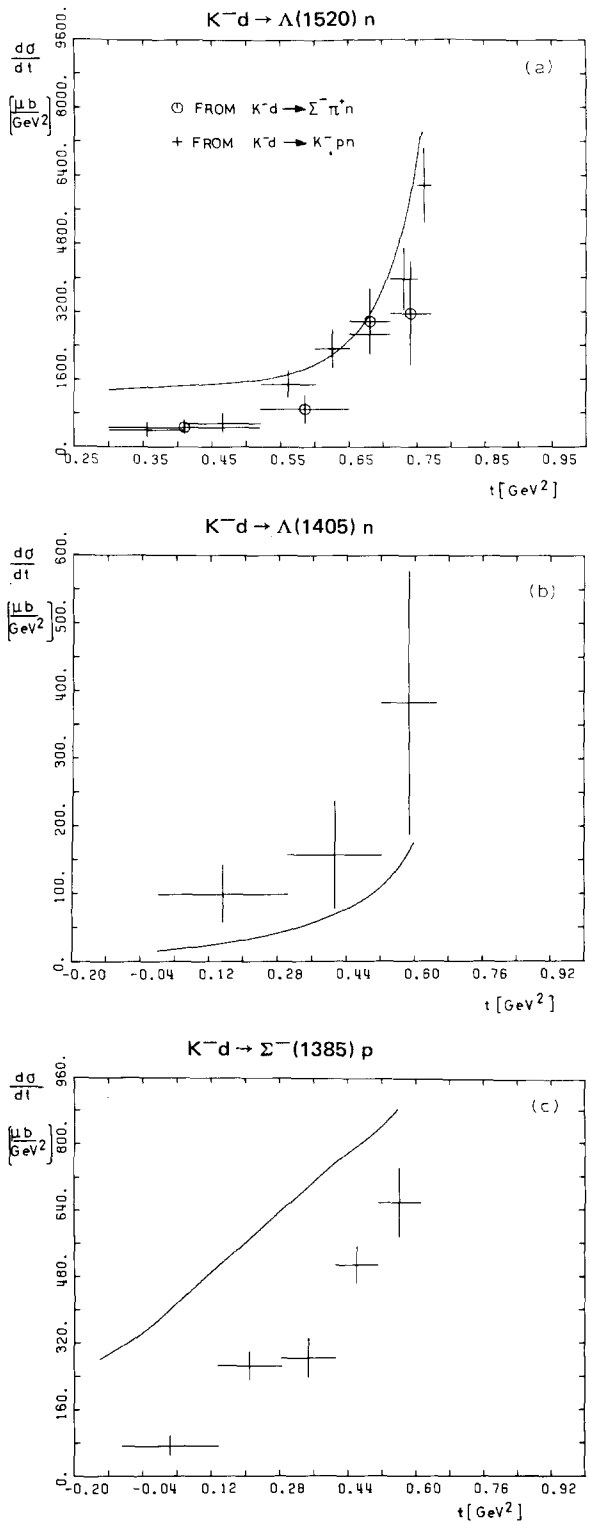
K⁻d → Λ(1520) n
(a)
⊙ FROM K⁻d → Σ⁻π⁺n
+ FROM K⁻d → K⁻pn
dσ/dt [μb/GeV²]
t[GeV²]
K⁻d → Λ(1405) n
(b)
t [GeV²]
K⁻d → Σ⁻(1385) p
(c)
t [GeV²]

Fig. 4.

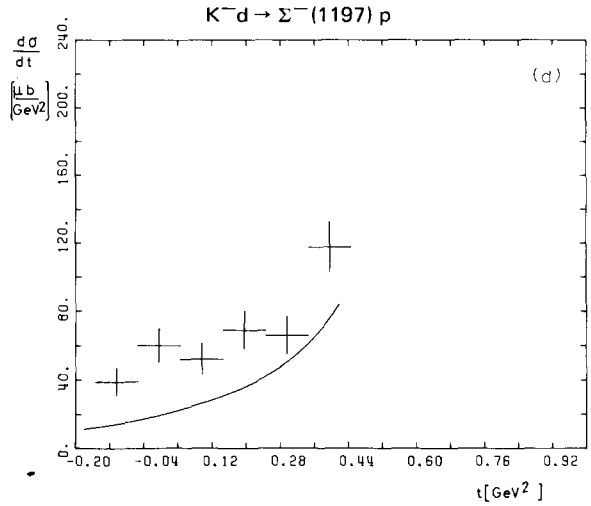

Fig. 4. Differential cross sections $d\sigma/dt$ as determined by the fits described in sect. 2.5 for the reactions (a) $K^-d \to \Lambda(1520)n$; (b) $K^-d \to \Lambda(1405)n$; (c) $K^-d \to \Sigma^-(1385)p$; (d) $K^-d \to \Sigma^-(1197)p$. The solid curves are calculated with the ONE model using the Reid [6] (soft core) deuteron wave function and the coupling constants: $g^2/4\pi(K^-p\Lambda(1520)) = 39\ GeV^{-2}$, $g^2/4\pi(K^-p\Lambda(1405)) = 0.04, g^2/4\pi(K^-n\Sigma^-(1385)) = 4.2\ GeV^{-2}$ and $g^2/4\pi(K^-n\Sigma^-(1197)) = 0.3$ (see table 5).

4. The one-nucleon-exchange model

In order to get an estimate for the $\bar{K}NY$ coupling constants we consider the one-nucleon pole contributions to the reaction $\bar{K}d \to Yp$ represented by the following graph:

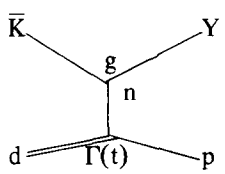

$$t = (d - p)^2$$
$$s = (d + \bar{K})^2$$

The general form of the npd vertex with the neutron off mass shell is

$$\Gamma(t) = F(t)\,\gamma\xi + G(t)\,p\xi + (\not{d} - \not{p} - m)(H(t)\,\gamma\xi + I(t)\,p\xi)\,,$$

where d and p are the four-momenta of the deuteron and the nucleon, the γ's are the Dirac matrices and $\not{p}$ and $\not{d}$ are $\gamma^\mu p_\mu$ and $\gamma^\mu d_\mu$ respectively. ξ is the polarization vector of the deuteron and m is the nucleon mass. In the present calculations we keep only the F- and G-terms since the contributions from the other two terms vanish at the nucleon pole.

The $\bar{K}NY$ coupling is taken from the following Lagrangians:

If the hyperon has $J = \frac{1}{2}$

$$L = g_{\bar{K}NY}(\bar{\psi}^{Y}\,\eta^{\pm}\,\psi^{n})\,\phi_{\bar{K}}\,, \qquad \begin{aligned} \eta^{+} &= i\gamma_5 \quad \text{for } P = +1\,, \\ \eta^{-} &= 1 \quad \text{for } P = -1\,; \end{aligned}$$

and if $J = \frac{3}{2}$

$$L = ig_{\bar{K}NY}(\bar{\psi}^{Y^{\mu}}\eta^{\pm}\,\psi^{n})\,\delta_{\mu}\phi_{K}\,, \qquad \begin{aligned} \eta^{+} &= 1 \quad \text{for } P = +1\,, \\ \eta^{-} &= i\gamma_5 \quad \text{for } P = -1\,. \end{aligned}$$

ψ^{Y}, $\psi^{Y^{\mu}}$, ψ^{n} are the fermion fields of the $\frac{1}{2}$ or $\frac{3}{2}$ hyperon and the nucleon respectively, $\phi_{\bar{K}}$ is the $\bar{K}$ meson field.

The cross section resulting from the amplitude corresponding to the above graph is

$$\frac{d\sigma}{dt} = \frac{1}{(s - M_D - \mu_K^2) - 4M_D\mu_K^2}\;\frac{g_{\bar{K}NY}^2}{4\pi}\;\frac{1}{(t - m^2)^2}\;S$$

$$\times\,\{\,|F(t)|^2\,Y_F + 2\,\mathrm{Re}(F(t)\,G(t)^*)\,Y_{FG} + |G(t)|^2\,Y_G\,\}$$

with

$$Y_F = (\Delta^2 - \mu_K^2)(\tfrac{1}{2}M_D^2 + \tfrac{2}{3}\alpha^2)$$

$$+ \tfrac{1}{3}(t - m^2)(\tfrac{3}{2}M_D^2 + \mu_K^2 - s + \Delta^2 - m_Y^2 - m^2 + 2\alpha^2)$$

$$+ \tfrac{1}{3}(t - m^2)^2\left(-1 + \frac{s}{2M_D^2} - \frac{\Delta^2}{2M_D^2}\right),$$

$$Y_{FG} = \tfrac{1}{3}\Bigg\{-2\alpha^2 m(\Delta^2 - \mu_K^2)$$

$$+ (t - m^2)(-\alpha^2\Delta + \tfrac{1}{4}m(M_D^2 - s - 4\Delta^2 + 3\mu_K^2 + 2m_Y^2 - 2m^2))$$

$$+ \frac{(t - m^2)^2}{4M_D^2}(m(2\Delta^2 - s - \mu_K^2) - M_D^2(2\Delta + m)) + \frac{(t - m^2)^3}{4M_D^2}\Delta\Bigg\},$$

$$Y_G = \tfrac{1}{3}\Bigg\{2\alpha^4(\Delta^2 - \mu_K^2) - (t - m^2)^4/(8M_D^2)$$

$$- \tfrac{1}{2}\alpha^2(t - m^2)(M_D^2 - s - 4\Delta^2 + 3\mu_K^2 + 2m_Y^2 - 2m^2)$$

$$+ \frac{(t - m^2)^2}{4M_D^2}(2\alpha^2(M_D^2 - \Delta^2 + \mu_K^2) - M_D^2(M_D^2 - s + \mu_K^2 - 2m^2 - 2\Delta^2 + 2m_Y^2))$$

$$+ \frac{(t - m^2)^3}{8M_D^2}(3M_D^2 - s + \mu_K^2 - 2\Delta^2 - 2m^2 + 2m_Y^2)\Bigg\},$$

where

μ_K = kaon mass , M_D = deuteron mass , m_Y = hyperon mass ,

$$\Delta = m + M_Y \qquad \text{with } M_Y = \begin{cases} m_Y & \text{for } J^P = \frac{1}{2}^- \text{ or } \frac{3}{2}^+ \\ -m_Y & \text{for } J^P = \frac{1}{2}^+ \text{ or } \frac{3}{2}^- \end{cases},$$

$$\alpha^2 = m^2 - \tfrac{1}{4} M_D^2 ,$$

$$S = 1 \text{ for } J = \tfrac{1}{2} ,$$

$$S = \{(m_Y^2 + \mu_K^2 - m^2 - (t - m^2))^2 - 4\mu_K^2 m_Y^2\}/6m_Y^2 \qquad \text{for } J = \tfrac{3}{2} .$$

In the non-relativistic limit the npd couplings $F(t)$ and $G(t)$ are connected with the non-relativistic wave functions of the deuteron by (see e.g. ref. [4]):

$$F(t) = \sqrt{2\pi/m}\,(m^2 - t)\{\tilde{u}(p) + \sqrt{\tfrac{1}{2}}\,\tilde{w}(p)\}$$

$$G(t) = \sqrt{2\pi/m}\,(m^2 - t)\left\{-\frac{3m}{p^2\sqrt{2}}\,\tilde{w}(p) + \frac{1}{2m}\,(\tilde{u}(p) + \sqrt{\tfrac{1}{2}}\,\tilde{w}(p))\right\}$$

with

$$\tilde{u}(p) = \frac{1}{p}\int u(r)\sin(pr)\,\mathrm{d}r ,$$

$$\tilde{w}(p) = \frac{1}{p}\int w(r)\,[\sin(pr) + 3\cos(pr)/(pr) - 3\sin(pr)/(pr)^2]\,\mathrm{d}r .$$

$u(r)$ and $w(r)$ are the radial wave functions of the deuteron for the S- and D-waves with $\int\{u^2(r) + w^2(r)\}\,\mathrm{d}r = 1$.

5. The kaon-hyperon-nucleon coupling constants

In the preceeding section we presented a formalism which allows the calculation of the one-nucleon exchange contribution to the cross section of reactions (1)–(4) as a function of t for a given coupling at the kaon-nucleon-hyperon vertex. This t-dependence of the cross section is precise only in the vicinity of the pole, that is for $t \approx m^2$. For physically accessible t values the extrapolation of the deuteron form factor $\Gamma(t)$ by means of deuteron wave functions is rather uncertain.

Still more important is the lack of knowledge about other possible contributions to reactions (1)–(4). They are negligible at the pole $t = m^2$ but may exceed the one-nucleon-exchange contribution for small t-values, since they are not expected

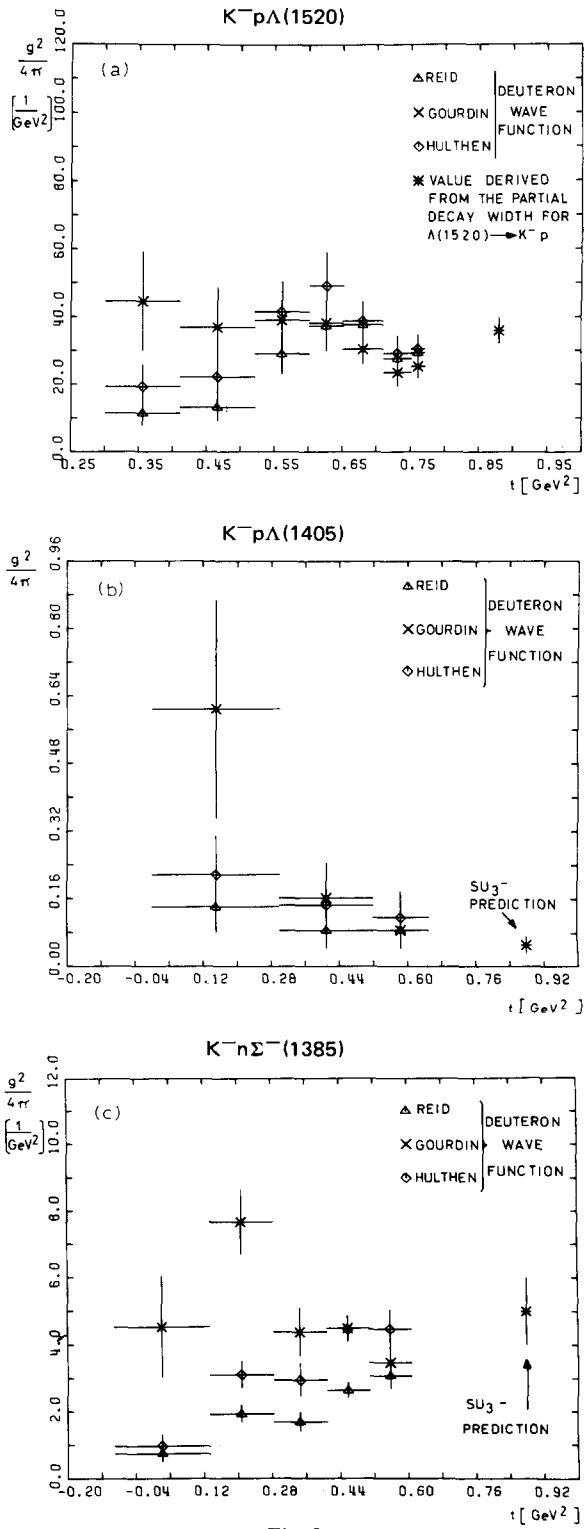
K⁻pΛ(1520)
(a)
REID
GOURDIN
HULTHEN
DEUTERON WAVE FUNCTION
VALUE DERIVED FROM THE PARTIAL DECAY WIDTH FOR Λ(1520)→K⁻p
t [GeV²]
K⁻pΛ(1405)
(b)
REID
GOURDIN
HULTHEN
DEUTERON WAVE FUNCTION
SU3 PREDICTION
t [GeV²]
K⁻nΣ⁻(1385)
(c)
REID
GOURDIN
HULTHEN
DEUTERON WAVE FUNCTION
SU3 PREDICTION
t [GeV²]

Fig. 5.

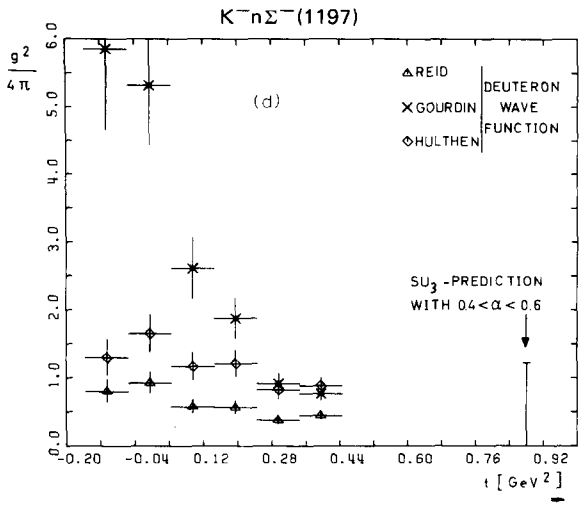

Fig. 5. Results for $(g^2/4\pi)_{\bar{K}NY}$ as a function of the four-momentum transfer squared $t = (K - Y)^2$. (a) $K^-p\Lambda(1520)$; (b) $K^-p\Lambda(1405)$; (c) $K^-n\Sigma^-(1385)$; (d) $K^-n\Sigma^-(1197)$. The results are obtained with the deuteron wave functions of Reid [6] (soft core), Gourdin [4] and Hulthén (hard core) [5]. At $t = m^2 = 0.88$ GeV^2 the expected values are indicated by *.

to fall off as rapidly as the one pole contribution. Thus a determination of the kaon-nucleon-hyperon coupling constants by the method described in sect. 4 should be based on an extrapolation in t to the pole at $t = m^2$.

We present our results on the $\bar{K}NY$ coupling constants in fig. 5, where we plotted as a function of t the "nominal" coupling constants, which are defined as the quotient of the measured differential cross section and the contribution of the one-nucleon-exchange term with $g^2/4\pi(\bar{K}NY) = 1$. The latter was calculated for 3 different deuteron wave functions: the relativistic generalisation of the Hulthén wave function with a hard core of 0.1 fermi (◇) [5], a phenomenological form factor (×) proposed by Gourdin et al. [4] and that by Reid using a soft-core potential (Δ) [6]. The extrapolation of the three resulting distributions in each diagram of fig. 5 to $t = m^2$ (= 0.88 GeV^2) should lead to the same value of the corresponding coupling constant.

The ranges of possible values of the coupling constants were obtained by an extrapolation of the distributions in figs. 5a–d. We attempted to find approximate minimum and maximum values compatible with the distributions in t of the "nominal" coupling constants. The corresponding numbers are listed in table 5.

We know from electron-deuteron scattering data that the Reid wave function [6] fits these data rather well even for large negative t-values [9]. From fig. 5 it can be seen that the values of the "nominal" $g^2/4\pi$ as determined with the Reid wave function is fairly linear with t. Since we know of no prescription how to extrapolate the "nominal" coupling constants to the pole position, we take this finding as the justi-

Table 5
Results for the kaon-nucleon-hyperon coupling constants

Coupling constant	Result from this experiment [a]	SU(3) prediction	Results from other experiments	Ref.
$\frac{g^2}{4\pi}(\bar{K}N\Lambda(1520))$	$60 \pm 20\ \mathrm{GeV}^{-2}$ $(78 \pm 8\ \mathrm{GeV}^{-2})$		$72 \pm 8\ \mathrm{GeV}^{-2}$ from partial decay width for $\Lambda(1520) \to \bar{K}N$	[3]
$\frac{g^2}{4\pi}(\bar{K}N\Lambda(1405))$	0.20 ± 0.15 (0.08 ± 0.16)	$\frac{2}{3}\frac{g^2}{4\pi}(\Lambda(1405) \to \Sigma\pi)$	$(1.7\text{–}4.1)\frac{g^2}{4\pi}(\Lambda(1405) \to \Sigma\pi) = 0.27\text{–}0.64$	[17]
		$= 0.10 \pm 0.02$	$\sim 8\frac{g^2}{4\pi}(\Lambda(1405) \to \Sigma\pi) = 1.25$	[10]
			very small	[16]
			$<<1$	[15]
$\frac{g^2}{4\pi}(\bar{K}N\Sigma(1385))$	$4.5 \pm 1.5\ \mathrm{GeV}^{-2}$ $(4.2 \pm 0.5\ \mathrm{GeV}^{-2})$	$\frac{2}{3}\frac{g^2}{4\pi}(\Sigma(1385) \to \Lambda\pi)$	$\sim -\frac{2}{3}\frac{g^2}{4\pi}(\Sigma(1385) \to \Lambda\pi) = 5.0\ \mathrm{GeV}^{-2}$	[11]
		$= 5.0 \pm 1.0\ \mathrm{GeV}^{-2}$	$\sim -\frac{g^2}{4\pi}(\Sigma(1385) \to \Lambda\pi) = 7.5\ \mathrm{GeV}^{-2}$	[10]
$\frac{g^2}{4\pi}(\bar{K}N\Sigma(1187))$	0.30 ± 0.25	$2(2\alpha - 1)^2\frac{g^2}{4\pi}(NN\pi)$	$\lesssim 6$	[12]
		$= 1.15$ (for $\alpha = 0.6$ (SU(6))	~ 28	[13]
			$\sim 3.2 \pm 0.6$	[14]
		$= 0.29$ (for $\alpha = 0.45$ or $\alpha = 0.55$)		

[a] The values in brackets are the results from a linear extrapolation to the nucleon pole (see sect. 5).

fication for a more quantitative determination of the kaon-nucleon-hyperon coupling constants by means of a linear fit, which extrapolates the nominal $g^2/4\pi$ (determined with the Reid wave function) to $t = m^2$.

The solid lines in fig. 4 show the ONE model contribution to $d\sigma/dt$ calculated with the Reid wave function and the fitted coupling constants, which are listed in table 5. The shape of the experimental distributions is well reproduced. However the predicted and measured cross sections differ considerably in size. This is no serious drawback since they are required to coincide only at the pole (i.e. for $t = m^2 = 0.88$ GeV^2). For the reaction $K^-d \to \Sigma^-(1197)p$ no fit has been performed because the experimental data are so far from the pole that a linear extrapolation to the nucleon pole does not seem reasonable.

In this context it is worth noting that in the t-regions where the Y resonances dominate, the polar and azimuthal decay angular distributions of the Y's in the Jackson frame have been found to be compatible with the predictions of the ONE model.

6. Discussion

The exact coupling constant for the $K^-p\Lambda(1520)$ vertex can be derived * from the decay of the $\Lambda(1520)$ hyperon into K^-p. The experimental values for the partial decay width as given in ref. [3] (PDG 76) yield:

$$g^2/4\pi(K^-p\Lambda(1520)) = 36 \pm 4(\text{GeV}^{-2}).$$

In the preceeding chapter we found for this coupling constant values in the range of 20 to 40 GeV^{-2}, which agrees well with the above result. This agreement suggests that our method to determine the kaon-nucleon-hyperon coupling constants using K^-d reactions and a ONE model is reliable to at least a 50% level, which is comparable to the precision of SU(3) predictions for the kaon-nucleon-hyperon coupling constants from other decay channels [7,8]. These predictions together with other experimental and theoretical results are listed also in table 5, where the following definitions have been used:

$$g^2(\bar{K}N\Lambda(1520)) = 2g^2(K^-p\Lambda(1520)),$$

$$g^2(\bar{K}N\Lambda(1405)) = 2g^2(K^-p\Lambda(1405)),$$

$$g^2(\bar{K}N\Sigma(1385)) = g^2(K^-n\Sigma^-(1385)),$$

$$g^2(\bar{K}N\Sigma(1197)) = g^2(K^-n\Sigma^-(1197)) \text{ **}.$$

* The relation between g and the partial decay width Γ of the Y's following from the Lagrangians given in sect. 4 are: $\Gamma = (g^2/4\pi)\,(p/m)\text{BF}$ with the barrier factor $\text{BF} = E \mp m$ for $J^P = \frac{1}{2}^{\pm}$ and $\text{BF} = \frac{1}{3}p^2(E \pm m)$ for $J^P = \frac{3}{2}^{\pm}$. p and E are the momentum and the energy of the decay baryon (with mass m) in the Y rest frame.

** This definition differs by a factor of 2 from the one used in ref. [7].

SU(3) predicts for $g^2/4\pi(\bar{K}N\Lambda(1405))$ a very small coupling constant, which is consistent with our findings but definitely smaller than what is found in ref. [10].

Our result for the $\bar{K}N\Sigma(1385)$ coupling constant is compatible with the SU(3) prediction and other estimates given in refs. [10,11]. For the coupling constant $g(\bar{K}N\Sigma(1197))$ we find a value which is compatible with the SU(3) prediction while the values given in refs. [13,14] are bigger.

We wish to thank our scanning and measuring staffs for their continued efforts in this experiment. We are grateful to N. Schmitz and K. Tittel for informative discussions and their support.

References

[1] V. Hepp, O. Braun, H.J. Grimm, H. Ströbele, C. Thöl, T.J. Thouw, D. Capps, F. Gandini, C. Kiesling, D.E. Plane and W. Wittek, Nucl. Phys. B115 (1976) 82.
[2] J.M. Blatt, V.F. Weisskopf, Theoretical nuclear physics (Wiley, New York, 1952).
[3] Particle Data Group, Rev. Mod. Phys. 48 (1976) no. 2, part II.
[4] M. Gourdin, M. le Bellac, F.M. Renard and J. Tran Thanh Van, Nuovo Cim. 37 (1965) 524.
[5] L. Hulthén and M. Sugawara, Handbuch der Physik, Bd. 39 (Springer, Heidelberg, 1957).
[6] R.V. Reid Jr., Ann. of Phys. 50 (1968) 411.
[7] M.M. Nagels, J.J. De Swart, H. Nielsen, G.C. Oades, J.L. Petersen, B. Tromberg, G. Gustafson, A.C. Irving, C. Jarlskog, W. Pfeil, H. Pilkuhn, F. Steiner and L. Tauscher, Nucl. Phys. B109 (1976) 1.
[8] N.P. Samios, M. Goldberg and B.T. Meadows, Rev. Mod. Phys. 46 (1974) 1.
[9] J.E. Ellias, J.I. Friedmann, G.C. Hartmann, H.W. Kendall, P.N. Kirk, M.R. Sogard, L.P. van Speybroek and J.K. de Pagter, Phys. Rev. 177 (1969) 2075.
[10] R.D. Tripp, R.O. Bangerter, A. Barbaro-Galtieri and T.S. Mast, Phys. Rev. Lett. 21 (1968) 1721.
[11] K.O. Bunnell, D. Cline, R. Laumann, J. Mapp and J.L. Uretsky, Nuovo Cim. Lett. 3 (1970) 224.
[12] N.M. Queen, M. Restignoli and G. Violini, Fortschr. der Phys. 21 (1973) 569.
[13] SABRE Collaboration, R. Barloutaud, D. Merrill, J.C. Scheuer, A.M. Bakker, W. Hoogland, S. Focardi, A. Minguzzi-Ranzi, A.M. Rossi, B. Haber, U. Karshon, J. Goldberg, G. Lamidey and A. Rouge, Nucl. Phys. B26 (1971) 557.
[14] S. Dubnicka, O.V. Dumbrajs and M. Staszel, Nucl. Phys. B88 (1975) 477.
[15] J.K. Kim, Phys. Rev. Lett. 19 (1967) 1074.
[16] D. Cline, R. Laumann and J. Mapp, Phys. Lett. 35B (1971) 606; Phys. Rev. Lett. 26 (1971) 1194.
[17] A.D. Martin and G.G. Ross, Nucl. Phys. B16 (1970) 479;
J. Thompson, Proc. Duke Conf. on hyperon resonances (1970) p. 61;
D. Berley, P. Yamin, R. Kofler, A. Mann, G. Meisner, S. Yamamoto, J. Thompson and W. Willis, Phys. Rev. D1 (1970) 1996.(E: Phys. Rev. D3 (1970) 2297);
Y.A. Chao, R.W. Kraemer, B.R. Martin and D.W. Thomas, Nucl. Phys. B56 (1973) 46;
A. Barbaro-Galtieri, Proc. Erice Summer School (1971) p. 581.